Developmental Biology ■ (■■■■) ■■■–■■■

Contents lists available at ScienceDirect

Developmental Biology

journal homepage: www.elsevier.com/locate/developmentalbiology

Follicle dynamics and global organization in the intact mouse ovary

Mehlika Faire [a,1], Amanda Skillern [a,1], Ripla Arora [a], Daniel H. Nguyen [a], Jason Wong [b], Chester Chamberlain [b], Michael S. German [b], Jennifer C. Fung [a], Diana J. Laird [a,*]

[a] Department of Ob/Gyn and Reproductive Sciences, Center for Reproductive Sciences, Eli and Edythe Broad, Center for Regeneration Medicine & Stem Cell Research, United States

[b] Diabetes Center UCSF, 35 Medical Center Way, San Francisco, CA 94043, United States

ARTICLE INFO

Article history:
Received 24 December 2014
Received in revised form
23 March 2015
Accepted 8 April 2015

keywords:
Whole tissue labeling
Confocal imaging
Ovary
Primordial follicle
Pancreas
Islet of Langerhans

ABSTRACT

Quantitative analysis of tissues and organs can reveal large-scale patterning as well as the impact of perturbations and aging on biological architecture. Here we develop tools for imaging of single cells in intact organs and computational approaches to assess spatial relationships in 3D. In the mouse ovary, we use nuclear volume of the oocyte to read out quiescence or growth of oocyte–somatic cell units known as follicles. This in-ovary quantification of non-growing follicle dynamics from neonate to adult fits a mathematical function, which corroborates the model of fixed oocyte reserve. Mapping approaches show that radial organization of folliculogenesis established in the newborn ovary is preserved through adulthood. By contrast, inter-follicle clustering increases during aging with different dynamics depending on size. These broadly applicable tools can reveal high dimensional phenotypes and age-related architectural changes in other organs. In the adult mouse pancreas, we find stochastic radial organization of the islets of Langerhans but evidence for localized interactions among the smallest islets.

Introduction

Recent advances in biological imaging and 3D analysis enable visualization of entire embryos and organs at subcellular resolution. The synthesis of microscopic detail at a macroscopic level is a revealing feature of tissue architecture such as cell orientation and cell shape as they relate to global properties such as morphogenesis (Le Garrec et al., 2013; Veeman and Smith, 2012). Comparison of such phenotypes across development, genetic backgrounds and different environments will begin to link tissue architecture to mechanism. Technical obstacles to wholemount imaging include penetration of the tissue with fixative and fluorescent labeling agents, optical clearing, and digital selection of the structures of interest in 3D reconstructed images. Algorithms have been developed for wholemount analysis of branching structures such as the kidney glomeruli (Short et al., 2014), but not for discrete units such as ovarian follicles.

Study of the ovary has been limited by information that can be obtained from histologic sections and the associated labor-intensive processing. Female reproductive lifespan and ovarian function depend upon the reserve oocyte population. Oocyte–somatic cell complexes termed primordial follicles (PFs) are established perinatally in mice with the encapsulation of a meiotically-arrested oocyte by an epithelial layer of granulosa cells (Pepling and Spradling, 2001). Activation of cohorts of PFs for growth begins immediately following their formation, with the proliferation of granulosa cells and concomitant expansion of the oocyte. Although it remains unclear whether oocyte or granulosa cells initiate growth (Hirshfield, 1992), morphometric analyses of mice and humans have revealed an increase in the diameter of the oocyte as well as the oocyte nucleus accompanying PF activation and early growth (Moore et al., 1974; Westergaard et al., 2007). Folliculogenesis progresses through primary, secondary and pre-antral stages and, before puberty, culminates in follicle demise; thereafter, endocrine signals cyclically rescue further follicle growth and promote meiotic resumption and ovulation (McGee and Hsueh, 2000). When the number of remaining PFs falls below a critical threshold, ovulation ceases and menopause ensues (Gosden et al., 1983; Richardson et al., 1987). Exhaustion of the ovarian reserve depends upon multiple factors: initial endowment of follicles, rate of their loss, and rate of follicle activation (Nelson et al., 2013). Despite the importance of the quiescent PF reserve to fertility and ovarian function, clinical assessment is indirect, using growing antral follicle counts and levels of hormones produced by the pituitary and granulosa cells as proxies (Rosen et al., 2012). Experimentally, the number of PFs is estimated in adults by manual counting in selected

* Corresponding author.
E-mail address: diana.laird@ucsf.edu (D.J. Laird).
[1] These authors have contributed equally.

http://dx.doi.org/10.1016/j.ydbio.2015.04.006
0012-1606/

histologic sections and applying a multiplication constant (Bristol-Gould et al., 2006a, 2006b).

Here we developed methodology to image oocytes in the intact mouse ovary using wholemount immunofluorescence. We use oocyte nuclear volume to distinguish non-growing from growing follicles and obtain absolute counts as well as early follicle growth dynamics. We develop approaches for spatial analysis and extend previous observations on the global patterning of quiescent and activated zones, which is established in neonatal ovaries; although this architecture endures throughout life, we find localized clustering of primordial and early growing follicles that increases in magnitude during aging. These approaches can be extended to other organ systems with a variety of markers, as we demonstrate in the adult mouse pancreas by imaging the islets of Langerhans.

Results

Identification of primordial and growing follicles by nuclear volume in intact ovaries

We established permeabilization and optical clearing parameters in wholemount mouse ovaries using DNA stains. We then screened oocyte-specific antibodies using these conditions. Nuclear antigens were preferred for their resolvability in 3D imaging, and the previously established expansion of the oocyte nucleus with early follicle growth suggested that nuclear volume could be used to distinguish non-growing from growing follicles (Moore et al., 1974; Fig. S1). In wholemount ovaries at postnatal day one (PD1), immunolabeling with the oocyte-specific transcription factor Nobox appeared variable, with larger and more robustly stained objects deepest in the ovary (Fig. 1A); this staining pattern was consistent with the reported onset of Nobox expression in late fetal oocytes (Suzumori et al., 2002; Rajkovic et al., 2004). A different distribution was observed at PD1 with the marker Germ Cell Nuclear Antigen (GCNA), which labels pre-diplotene oocytes at the periphery of the neonatal ovary (Enders and May, 1994; Kerr et al., 2006): a shell of GCNA$^+$ cells surrounded a concentration of Nobox$^+$ cells at the center of PD1 ovaries (Fig. 1B). By PD5, the majority of oocytes are incorporated in follicles (Pepling, 2006) and accordingly we observed NOBOX immunofluorescence more uniformly throughout the ovary, with individually-labeled cells readily separable in 3D reconstructions of confocal stacks (Figs. 1C, S2A). Thus wholemount staining of the neonatal ovary recapitulates the temporal and spatial dynamics of a nuclear marker of meiotic prophase marker (GCNA) and the Nobox homeobox transcription factor, which is required for the postnatal differentiation of oocytes and folliculogenesis (Rajkovic et al., 2004).

Volumes of objects defined by NOBOX and GCNA immunostaining were examined in frequency distribution. At PD1, near the onset of follicle formation (Pepling, 2006), comparison of these profiles reveals similar range of sizes but smaller average volume of Nobox$^+$ objects (Fig. 1D); this difference, together with the shoulder in Nobox distribution above 1500 μm^3 may reflect the earliest wave of NOBOX expression. As only oogonial cysts and PFs are present at PD1 (Pepling and Spradling, 2001), we used this timepoint to set an upper limit for detectable Nobox volumes. A threshold of 3000 μm^3 for PF nuclei was rationalized, as this includes $>$99.5% of both GCNA and Nobox volumes at PD1. Measurements of oocyte nuclear volume in PFs from thick histologic sections revealed a similar distribution: a mean of 1169 μm^3 and

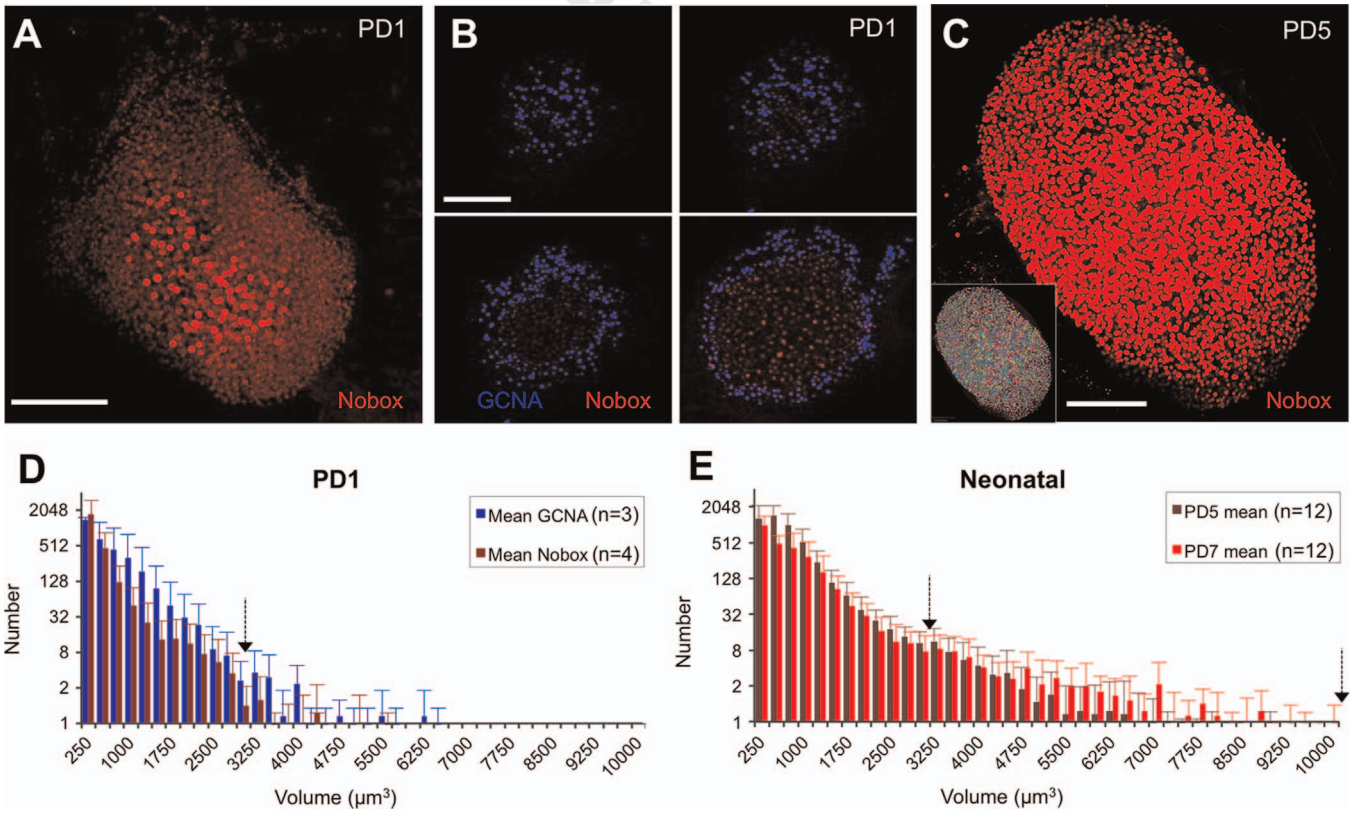

Fig. 1. Oocyte nuclear markers enable spatial resolution of follicles in wholemount neonatal mouse ovaries. Extended projections of Nobox immunostaining in an intact PD1 ovary (A). Optical *z* stack slices through a PD1 ovary stained with Nobox (red) and GCNA (blue) show surface localization of the GCNA+ cells and exclusive Nobox$^+$ cells in the core (B). Extended z-stack projection of Nobox staining in an intact PD5 ovary (C). Selection of Nobox$^+$ objects is indicated by separate colors, inset. Frequency distribution of Nobox volumes compared with GCNA at PD1 (D) shows cutoff for PFs at 3000 μm^3. Comparison of Nobox frequency distributions reveals a stepwise increase of largest object sizes from birth to PD5 to PD7 by the lengthening of the right tail, and a concomitant loss of smallest objects (E). Scale bars represent 150 μm.

Please cite this article as: Faire, M., et al., Follicle dynamics and global organization in the intact mouse ovary. Dev. Biol. (2015), http://dx.doi.org/10.1016/j.ydbio.2015.04.006